

High-Speed 2x25kV Traction System Model and Solver for Extensive Network Simulations

Bassam Mohamed, *Member, IEEE*, Pablo Arboleya, *Senior Member, IEEE*,
Islam El-Sayed and Cristina González-Morán, *Senior Member, IEEE*

Abstract---In this work, a simplified model of a 2x25kV bi-level traction power system for feeding high-speed trains is presented. A Modified Nodal Analysis (MNA) based algorithm for solving the system with and adaptive damping factor is also explained. The main novelties of this work are the inclusion of train protections (over-current and over-voltage) in the model and the development of the MNA solving procedure that increases the stability and robustness of the iterative solving process. Another important feature of the model is that it can be easily adapted to a single voltage feeding systems by deactivation of specific parameters. The accuracy and performance of the proposed simulator is compared and verified relative to the derivative based solvers.

Index Terms---2x25kV AC railway, Adaptive Damping Factor, Backward/Forward Swept, High-Speed Railway, Modified Nodal Analysis, Newton-Raphson, Power Flow, Railways, Traction Power Systems.

I. INTRODUCTION

ACCORDING to the International Association of Public Transport (UITP) [1], 400 billion of trips are made each year in the European Union and 15% of those trips are made using public transport. Among those, 45% are made using railway systems. Railway transportation is recognized as the most environmental friendly form of mass transport with an average consumption of 0.12 kWh per passenger and kilometer and it is also the safest transportation system. Among all kind of railway transportation systems, high-speed railways (HSR) for connecting major cities became quite popular around the world with more than 8.9 billion of passengers each year and more than 38000km of electrification. China accounts for more than two-thirds of those kilometers and it will reach 30000km by 2020, but the degree of development of HRS is also very high in Europe (nearly 9000km) and in Japan. In other countries like United States and Australia the debate about these kind of transportation systems is already open.

In this context, the number of researchers working on this topic in the last years has grown in a significant way. Many efforts have been invested not only in the development of technologies applied to vehicles but also in the development of the power systems that feed them, that are an essential part of the the necessary infrastructure.

Many of the works presented in the last years were devoted to study the impact of new technologies in the traction network or

B. Mohamed, P. Arboleya, I. El-Sayed and C. González-Morán are with the Department of Electrical Engineering, University of Oviedo, Spain e-mail: arboleyapablo@uniovi.es

This work was partially supported by the Ministry of Science, Innovation and Universities through the CDTI strategic program CIEN (National Business Research Consortiums) under the granted project ESTEFI

Manuscript received XXX, 2018; revised XXX, 2018.

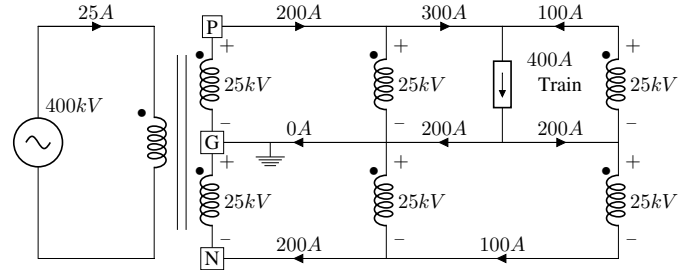


Fig. 1: 2x25kV AC traction section with two cells and a train placed at the second cell.

the impact of the traction network over the main distribution or transport grid. For instance, in [2], a methodology to optimize the off-board hybrid energy storage systems in AC rails is proposed. The same authors studied the effect of adding renewable generation inside the traction network in [3]. In [4], the traditional AC traction networks are replaced by 24kV DC traction systems using multilevel converters. [5] proposed the use of power electronic links between the neutral zones of 2x25kV AC traction systems to reduce the losses and the investment cost and [6] developed an optimization methodology to study the impact over the electrical grid of a railway corridor composed of 8 railway substations connected to the primary grid and 10 lines.

For carrying out the different studies, it is crucial the development of accurate and effective mathematical models of all elements present in the infrastructure. The degree of detail of the different models varies depending on their application. In the case of power quality studies, we can find very detailed models of the electrical infrastructure and the trains. Very good examples of the integration of a detailed model of train plus high speed infrastructure are the ones proposed in [7], [8], [9]. The model presented in [10] has been specifically designed for studying the problem of low frequency oscillations in traction networks.

A common feature of all of the above-mentioned models is that all of them are very complex and accurate models suitable for being used in transient simulations with a low number of lines and trains. However, they are not appropriate for planning purposes with long simulation periods and a large number of trains, lines and substations. For this kind of studies, simplified models solved using time-varying curves in quasi-static simulations are the more suitable. We can find in the literature many steady state models for DC traction systems [11], [12] and also for AC traction systems. As far as high speed systems are concerned there can be several types of feeding systems. An analysis of most of them can be found in [13]. By far the most common is the so called 2x25kV bi-level

power system like the one represented in Fig. 1. As it can be observed, the transformer connecting the AC traction system with the main grid has the secondary winding split in two, the central point (grounded) is connected to the rails while the other two points are connected to the overhead feeding system (catenary from now on) and the return conductor. By means of autotransformers, the sections are divided in different cells. A section is fed by a power transformer and the different sections are separated by dead-zones or neutral-zones. The train is electrically connected between the catenary and the rails. With this system, the energy is transported at 50kV in the cells without trains reducing the losses and the number of required substations.

This paper is going to be devoted to the development of a simplified model and a quasi-static solving procedure for this kind of system, but the same model can be used for single-voltage systems just by deactivation of some specific elements. It is not the first attempt or proposal to model and solve the 2x25kV networks. For instance, in [14], an equivalent monovoltage system of the classic 2x25kV system is proposed by using the Fortescue theorem. As the authors mentioned, the solution is elegant, accurate and it reduces the computation time but it is really complicated to use and it must be mentioned that it only works under the assumption that positive and negative catenaries are balanced, which could not be true in a general case. [15] used the Carson equations to model together the rails and the soil in a simplified manner. A modified current injection method for solving these kind of systems was presented in [16], and in [17], the authors used a backward/forward swept (BFS) method. In [18], the authors demonstrated that the BFS algorithm is faster than the conventional derivative based algorithms. However, BFS algorithms present serious convergence problems in the presence of non-reversible substations (in case of DC systems) and other non-smooth characteristic loads/generators, like for instance, trains with over-voltage and over-current protections.

The proposed model, unlike those discussed above, considers the use of an over-current and over-voltage protections in the trains and it is specially designed for being used in massive simulations with long simulation periods and a large number of trains and substations. The solver is based on a modified nodal analysis (MNA) algorithm with an adaptive damping factor making it much more stable and robust in terms of convergence but still much faster than those derivative based as it will be demonstrated. The paper is structured as follows. In the next section, the models of the different devices present in the network are described as well as the train model. The integration procedure of these devices and trains inside the network model is also explained in the next section. Section III describes the solving procedure. In section IV, a set of cases of study are presented and analyzed. Finally, in section V the conclusions are stated.

II. MATHEMATICAL MODEL

Through the different subsections of this section we will describe the different mathematical models of the devices present in the network and the trains. After that, we will describe how to integrate all of them within the network model.

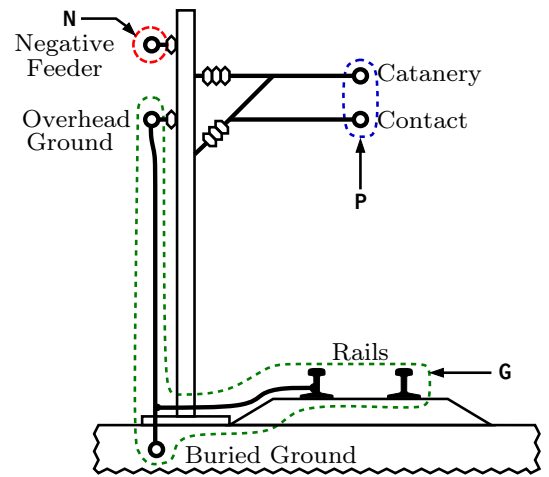


Fig. 2: The feeding system of 2x25 AC railways [19], [20]

To integrate all the equations in the system in a compact way, the connection matrix (Γ) described below is used repeatedly throughout the article. Γ is used to generate a linear combination from a given input vector. The element $\Gamma(m, n)$ represents the participation factor of input (n) in the output (m). The incidence matrix is a connection matrix where rows represent devices (line impedances, train, sources, ...) and columns represent nodes. All elements in Γ are cleared to zero except the elements of positive and negative nodes, that are set to 1 and -1 respectively as defined in Equation 1.

$$\Gamma(m, n) = \begin{cases} 1 & n = \text{Positive node of device } m \\ -1 & n = \text{Negative node of device } m \\ 0 & \text{otherwise} \end{cases} \quad (1)$$

For instance, the device voltage vector (V_d) and the injection current vector (I) contain respectively the voltage drop in all devices of the system and the current injected at each node. They can be calculated as a function of the nodal voltage vector (V) containing the voltage in all nodes of the system with respect to ground and the device current vector (I_d) containing the current through all devices respectively by means of the incidence matrix as shown in Equation 2 and Equation 3.

$$V_d = \Gamma \times V \quad (2)$$

$$I = \Gamma^T \times I_d \quad (3)$$

A. Catenary sections description

The wiring layout in 2x25kV system is quite complex and there are many conductors and electrical paths involved. A very detailed description of the system with all possible variations can be found in Chapter 4 of reference [21]. In Fig. 2, a simplified scheme is represented. In most of the cases, for describing the different feeder of the system in a simple way, a lumped model like the one proposed in [22] and [20] is used. The so called positive feeder (marked as P in Fig. 1 and Fig. 2) or overhead conductor is formed by the catenary plus the contact wire that are usually connected by droppers and switching wires. The ground path (marked as G in Fig. 1 and Fig. 4) is formed by the rails, the overhead and the buried ground

conductors. Finally, the return path, also called negative feeder for analogy with the DC systems (marked as N in Fig. 1 and Fig. 2) is formed by the return conductor. As it can be observed, the wires can be grouped creating three sets of conductors. The first set represents the positive feeder (P), the second set represents the ground feeder (G) and the third set represents the negative feeder (N). As it was demonstrated in [22] it is possible to reduce the whole system to a lumped parameters model using a reduction method based on the reduction of a group of conductors at the same potential to an equivalent conductor. This equipotential assumption holds for all cases where a set of conductors is bonded together like in the 2x25kV systems [22]. The obtained simplified lumped parameters model is formed by three longitudinal elements representing the inductances and resistances of the lines plus transversal resistive/capacitive elements. As it is demonstrated in this reference, the error obtained neglecting the resistive/capacitive transversal elements is less than 1%, so the system can be represented by three resistive/inductive longitudinal elements representing the self-impedances of the positive, ground and negative feeders plus the couplings between them, that can be considered purely inductive. This lumped parameter circuit or a small variation of it, is used for most of the researchers that develop power flow algorithms for these kind of systems. There are many researchers that also neglect the mutual impedances [23], [24], [25], [26], [14], [27], [28], [16], [5], [29], [30] simplifying the system to the limit removing the off diagonal terms of admittance matrix. The system is much lighter from the computational point of view, but the accuracy of the calculation is lower since the effect of the inductive couplings is not negligible. On the other side, many authors propose or use very complicated models considering the couplings as it can be observed for instance in [31], [32], [7], [8], [33], [19], [34]. These models are very accurate but also complex from the point of view of their computational burden, which is a very important drawback for making extensive calculations. The approach adopted by the authors is the one presented in [35], [20]. This approach considers the mutual couplings between the longitudinal elements, but taking advantage of the fact that the ratios between specific currents in the system are always real numbers since those currents are in phase or shifted 180 degrees. Using these current ratios is possible to reduce the system with couplings to an equivalent system using a modified set of the self-inductances. In this case and without losing any generality, we will use this approach that we will allow us to consider the couplings maintaining the simplicity of the mathematical model.

B. Substation Model

The traction substations connect the traction network with the main grid. Each substation includes a power transformer to adapt the HV at primary side to traction voltage at the secondary side. Very detailed substations models are proposed when the interaction between the railway feeding system and the grid is required as it can be observed for instance in [7], [8], but this is not what the authors try to model in the present work.

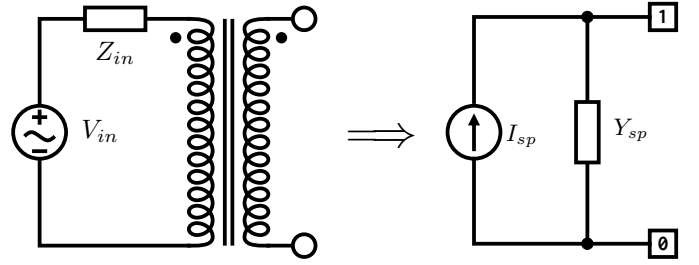


Fig. 3: Simulation model of a single supply substation

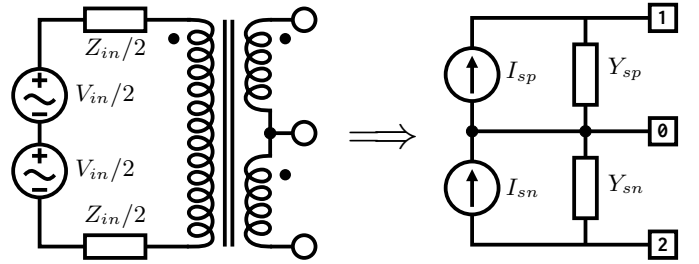


Fig. 4: Simulation model of a dual supply substation

In Fig. 3 and Fig. 4 (left), the electrical model of the traction substation for the single-voltage and bi-voltage cases are depicted respectively. The presented model is equivalent to the one using two voltage sources with series impedances which has been widely used by many authors, see for instance the references [22], [16], [25], [34], [33].

The high voltage side can be replaced by the Thévenin equivalent circuit to simplify the model. The series impedance (Z_{in}) at the primary side of the transformer is calculated based on the short circuit power of the substation and the leakage inductance of the transformer. An extra impedance to simulate the voltage drop in the transport network can be also added. In the case of single feeding system, the substation model can be simplified using the Norton equivalent circuit as shown in Fig. 3 (right). The current source based model is more suitable for the MNA algorithm because it provides a direct current injection in the node. In bi-voltage feeding systems, the primary side circuit can be divided symmetrically into two voltage sources and two series impedances. Fig. 4 (right) shows the simplified model obtained using the Norton equivalent of a bi-voltage feeding system substation. The midpoint between the two circuits is used as a ground reference. The voltage in the terminals of the current sources must be defined depending on the turn ration and in the general case, it should have the same value since turn ratios of both windings are generally equal.

We are going to refer to the no-load voltage between the terminals 1 and 0 as positive voltage (V_{sp}), and the no-load voltage between the terminals 0 and 2 as negative voltage (V_{sn}). Both voltages will be expressed in p.u. and they can be related by means of the turn ratio of their respective windings (N) as follows:

$$V_{sn} = V_{sp} / N \quad (4)$$

The primary to positive turn ratio (N_p) and the primary to

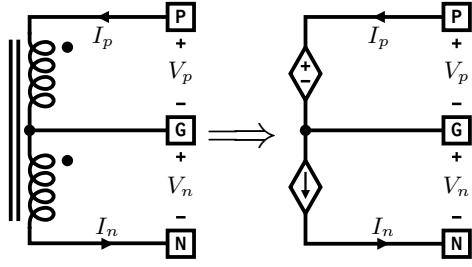


Fig. 5: Simulation model of autotransformer

negative turn ratio (N_n) can be obtained using

$$N_p = (V_{sp} \times V_b) / V_{in} \quad (5)$$

$$N_n = (V_{sn} \times V_b) / V_{in} \quad (6)$$

Where V_b is the base voltage in (V) and V_{in} is the voltage at the HV side of the substation in (V). The admittances Y_{sp} and Y_{sn} in p.u. of the equivalent current sources (see Fig. 3 and Fig. 4 (right)) are obtained by means of

$$Y_{sp} = Z_b / (Z_{in} \times N_p^2) \quad (7)$$

$$Y_{sn} = Z_b / (Z_{in} \times N_n^2) \quad (8)$$

Where Z_b represents the base impedance in (Ω). Using the previously defined impedances we can obtain the equivalent current sources in p.u. of the substation I_{sp} and I_{sn} .

$$I_{sp} = Y_{sp} \times V_{sp} \quad (9)$$

$$I_{sn} = Y_{sn} \times V_{sn} \quad (10)$$

We will define a vector I_c with n positions, being n the total number of nodes that will represent the nodal current injection of all constant sources. I_c will have all zeros except in the two first positions in which we will place $-I_{sp}$ and I_{sn} respectively.

C. Autotransformer Model

In bi-voltage feeding systems, each section (fed by a single substation) is divided into cells. A cell can be defined as the portion of the system located between two autotransformers or between an autotransformer and a substation. In all cases, an autotransformer is placed at the end of each cell (see Fig. 1). The autotransformer has two windings (positive and negative) and it is connected by three terminals (P,G and N) to the overhead feeder, the rails and the return conductor respectively (see Fig. 5 (left)). In most of the cases, the autotransformer has unitary turn ratio. In asymmetrical feeding systems, the negative voltage (V_n) maybe much higher than the positive voltage (V_p) to reduce the losses of the negative feeder. The model of an ideal autotransformer can be represented using two dependent sources, a voltage and a current source as shown in Fig. 5 (right). The leakage and magnetizing impedances of the autotransformer are neglected to simplify the model. The accuracy of the solution is acceptable because those impedances are around 1% [20], [35]. In case that the user wants to model a system with higher impedances, it would be recommended to include them in the model. The power transferred between the two windings is defined in Equation 11.

$$S = I_p^* \times V_p = -I_n^* \times V_n \quad (11)$$

All autotransformers in the system can be defined by means of two linear matrix equations, the voltage equation and the current equation. In this case N will represent a diagonal matrix with all autotransformer turn ratio. The voltage relation between positive and negative ports is defined by Equation 12. Each autotransformer adds its positive current (I_p) to the vector of unknowns which includes also the node voltages (V). The negative current (I_n) can be substituted by the positive current (I_p) using the Equation 13.

$$V_p = N \times V_n \quad (12)$$

$$I_n = -N \times I_p \quad (13)$$

The connections of autotransformers are represented by two incidence matrices. The first one (Γ_P) represents the positive windings connections on the top, while the connection of the negative windings are represented by (Γ_N). The voltage equation of the autotransformer expressed in Equation 12 can be expressed for all the autotransformers in the system using the nodal vector and the incidence matrix as follows:

$$0 = \Gamma_p \times V - N \times \Gamma_n \times V = C \times V \quad (14)$$

Where (C) is a constant matrix $C = \Gamma_p - N \times \Gamma_n$. Equation 14 is added to the mathematical model to compensate the additional unknowns added by I_p . The nodal injection current of the autotransformer (I_a) is defined also based on the positive port current (I_p) and the transpose of the (C) matrix as shown in Equation 15.

$$I_a = \Gamma_p^T \times I_p - \Gamma_n^T \times N \times I_p = C^T \times I_p \quad (15)$$

D. Train Model

The reference power profile (P_{ref}) of the train is given as an input for the simulator via a file called XTP generated by an external software containing a very detailed electro-mechanical model of the train. For each trip, the XTP file contains the position, the time respect to the start of the trip and the power reference. Each profile represents a single run of a train on a specific track which may consist of multiple of sections. A similar approach can be found in [14], [30], [29], [35], [31], [22], [33], [16], [34].

The distance of the XTP profile data must be consistent of the total length of the track. The simulator reads the XTP data and interpolate them on a fixed step time. The train is located on its section and cell based on its position relative to the track.

In Fig. 6, we can observe two different tracks, corresponding with the trip of two trains, the trip of train 1 from A to B (track 1) and the trip of train 2 from B to A (track 2). Both tracks have the same length of (52km) and both tracks goes through sections 1 and 2 that are fed by the same substation. Both sections have three cells of different lengths as expressed in the figure. We consider that a train moves forward in a section if it moves away from the substation that feeds that section, otherwise the train would be moving in a reverse direction inside this section. This is just a convention that we choose to define the movement of the trains within the system. As it

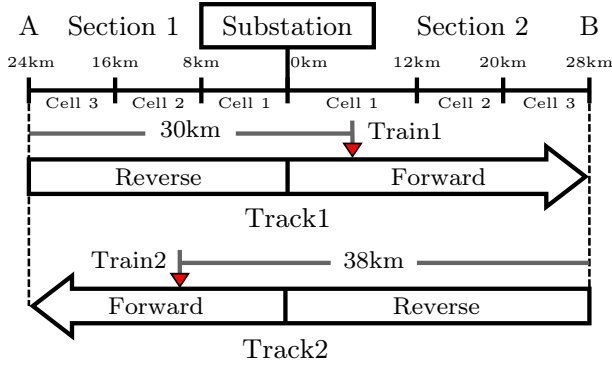


Fig. 6: Sections directions in dual track example

can be observed, for the track 1, the train will move first in reverse direction in section 1 and then in forward direction in section 2. For the track 2, the train will move first in reverse direction in section 2 and then in forward direction in section 1. If we consider that the train 1 in Fig. 6 is travelling from A to B (track 1) and it is placed at 30km from the beginning of its track (point A), this means that it is placed in the cell 1 of the section 2 at 6km from the beginning of the cell (the beginning of a cell is always the closest point to the substation within the cell). This is how the position that the algorithm will use to place the train in the system is defined, section 2, cell 1, position inside the cell 6km (0.5 pu). In the case of the train 2, it is in track 2 placed at 38km from B (starting point of its track), that means that the train is in section 1, cell 2 and position 2km (0.25pu) from the beginning of its cell.

The train is connected to the network by two nodes (positive and ground). The connection of all trains in the system is defined by the train incidence matrix (Γ_t). Each train is represented by a single row where the column of the positive node is set to 1 and the column of the negative node is set to -1.

The protection curves described in the following paragraphs allow us to simulate the trains control and their interaction with the network, the same approach has been widely used among the authors in DC railway systems, see for instance [11], [12] and we extended the technique in this paper to the AC railways systems. According to the standards IEC60850:2014 [36] and CENELEC-EN50163 [37], we can define V_1 , V_2 , V_3 and V_4 as the lowest non-permanent voltage, lowest permanent voltage, highest permanent voltage and highest non-permanent voltage respectively. Very low voltages must be avoided since the train would need to extract a very high current for a specific power damaging the power electronic equipment inside the train. Very high voltages could put in risk the isolation of the different devices of the infrastructure and also the trains. For

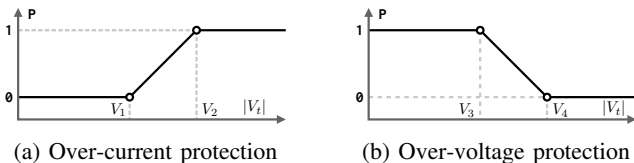


Fig. 7: Protection curves

that purpose, the trains are provided with a set of mechanisms that limit the current reducing the requested power in case of low voltage scenario. In the other hand, the regenerated power injected into the network should be also limited burning part of it in the rheostatic system in case of high voltage scenario. The protection curves represented in Fig. 6 summarize these overcurrent protection systems in low voltage scenarios and overvoltage protection systems in high voltage scenarios. Low voltage scenarios are usually connected with trains working in traction mode while high voltage scenarios usually imply a surplus of regenerated power.

The reference power of the train may be limited in traction or braking mode by the over-current and over-voltage protection respectively. The over-current protection shown in Fig. 7a is activated at low voltage profile, usually when the train is in traction mode absorbing power from the catenary. If the voltage magnitude is lower than (V_2), the train power is reduced linearly until it is blocked totally when the voltage magnitude is lower than (V_1). Fig. 7b shows the squeeze control which protects the system from over-voltage by limiting the regenerative braking power injected in the catenary when the voltage magnitude is higher than (V_3). For voltages higher than (V_4), the train can not inject any regenerated power into the catenary. The blocked power is derived and burned by the rheostatic braking system inside the train. Summarizing, the train power (P_t) can be obtained as a function of the power reference (P_{ref}), defined as an input in the XTP files and the catenary voltage as follows:

$$P_t = \mathcal{PV}(V_t, P_{ref}) \quad (16)$$

where the function \mathcal{PV} represents the protection curves previously defined. The simulator calculates the reference value of the reactive power assuming specified power factor. Equation 17 defines the (r_{qp}) as a ratio between reactive Q_t and reactive P_t powers for a given power factor PF.

$$r_{qp} = \sqrt{(PF)^{-2} - 1} \quad (17)$$

The train reactive power can be obtained as

$$Q_t = |P_t| \times r_{qp} \quad (18)$$

The train current is updated by Equation 19 based on the apparent power (S_t) and the voltage (V_t).

$$I_t = conj(S_t \oslash V_t) \quad (19)$$

The \oslash operator represent the phasor product. Finally, a vector with all voltages between the catenary and the rails for all trains can be obtained using Equation 20 and a vector with all nodal currents injected by the train can be computed using Equation 21.

$$V_t = \Gamma_t \times V \quad (20)$$

$$I_{nt} = \Gamma_t^T \times I_t \quad (21)$$

Fig. 8 shows the block diagram of the train model which updates the train current at each iteration of the solver.

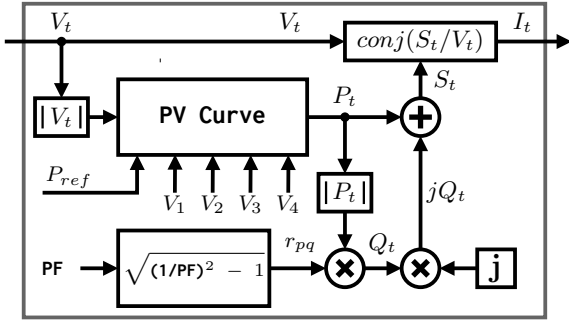


Fig. 8: Train current model based on protection curves

E. Network Model

The topology of the traction network is updated dynamically based on the position of all trains at each instant. The solver will divide the nodes in static and dynamic nodes. The static nodes include the terminals of the substations and autotransformers. We define the static lines as the connections between the static nodes assuming the network without trains. The dynamic network is reconstructed at each instant considering that the trains split the static lines depending on their position. For this purpose, an optimized line splitting procedure has been designed and implemented. The line splitting procedure divides the positive (catenary plus contact wire) and ground feeders (rails) into line segments. It must be pointed out that the return conductors remain always as a static lines.

For splitting a specific line, first trains are sorted and classified according to their position on the line starting from the source node. Then, trains are grouped and located at the existing static nodes or new dynamically created nodes. Finally, new dynamic lines are created by connecting the source and destination nodes with the new dynamic nodes. The distances from the source node are normalized relative to the line length so the destination node will be located always at 1. The length of line segments is limited to a minimum length (X_{Min}) to prevent from creating ill conditioned systems. The splitting algorithm may shift the trains to nearby nodes to avoid this condition. (X_{Min} must be less than half the length of the trains to ensure the accuracy of the solution. The variable (Pre) tracks the previous node number that is initialized as the source node, while the variable (Pre_X) stores its location. The previous node is the starting point of all segments. The last line segment ends with the destination node, while other intermediate segments end with new nodes. The algorithm adds the last line segment in all cases even when there are no trains. An intermediate line segment is added for the new node. The connections of the line segments are represented by the incidence matrix (Γ_L). Fig. 9 shows different cases faced by the line splitting algorithm depending on the train positions. The following paragraphs explain the case study shown in Fig. 9.

- 1) Train located near the source node (T_1): If the distance (X_1) is less than (X_{Min}), the train is shifted to the source node.
- 2) Train located far from any node (T_2): If the distance with the previous node (X_2) is greater than (X_{Min}), the

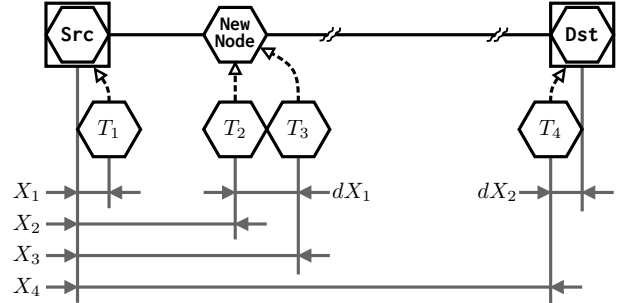


Fig. 9: Example of different cases of line splitting

train is located at a new node. A new line segment is added to connect the previous node with the new one.

- 3) Train located near the previous node (T_3): If the distance between the train and the previous node (dX_1) is less than the (X_{Min}), the train is located at the previous node.
- 4) Train located near the destination node (T_4): If the distance between the train and the destination node (dX_2) is less than the (X_{Min}), the splitting algorithm shifts the train to destination node.

III. SOLVING PROCEDURE

It must be remarked that, as it was previously mentioned, each substation can feed different sections that are separated from other sections fed by different substations by neutral zones without any electrical connection. The proposed simulator, labeled for commercial use as ACTS, solves each network fed by an individual substation independently in a sequential way but this process can be parallelized. Taking advantage of this feature, the speed of the solving procedure can be increased.

In all the representations in this paper, we will assume the positive current reference when the direction of the current is to the right part of the scheme. The voltage measurements are relative to the ground node. All currents and voltages are in rms value. The mathematical model is based on the MNA as defined in Equation 22. A similar approach was used to solve DC traction systems in [12]. However, in this case the solver is extended and modified in order to deal with complex variables and with the complex specific topology of the 2x25kV AC systems.

$$\begin{bmatrix} Y_n & C^T \\ C & 0 \end{bmatrix} \times \begin{bmatrix} V \\ I_p \end{bmatrix} = \begin{bmatrix} b \\ 0 \end{bmatrix} \quad \begin{array}{l} \text{KCL} \\ \text{Equation 14} \end{array} \quad (22)$$

The vector of unknowns (x) includes the voltage of all nodes (V) and the current of the positive part of the autotransformers (I_p). The equations of the mathematical model are classified into two groups. The first group represents the Kirchhoff's Current Law (KCL) at each node. The second group represents the voltage equation of the autotransformers (Equation 14). The nodal admittance matrix (Y_n) is used to model the constant admittance of the lines segments and shunt elements as defined in Equation 23. The (Y_n) matrix is built based on the line splitting procedure and it changes dynamically as the train

moves. However, the matrix (A) is constant during all iterations of a single instant of the simulation.

$$Y_n = \Gamma_L^T \times Y_L \times \Gamma_L + Y_{sh}, \quad (23)$$

Y_L is a diagonal matrix with the diagonal terms representing the admittances of the lines. Y_{sh} is also a diagonal matrix with terms in the diagonal representing all shunt admittances present in the system. I_b represents all current injections of the trains as well as the constant sources of the substations, it can be calculated as

$$I_b = I_c + I_{nt} \quad (24)$$

where (I_c) stands for the constant current of the substations and (I_{nt}) represents the nonlinear current of the trains.

We must emphasize that the line splitting algorithm is responsible for creating the dynamic node and line segments based on the position of the train. The impedance of the line segment is proportional to the segment length and the total impedance of the line. If the line segment is too short, the impedance will be a small value which leads to huge admittance. High variation in the admittances will produce ill-conditioned systems, so the solver needs to deal very carefully with this dynamic node creation in order to avoid this critical effect. In order to do overcome this problem the solver use the next strategy. The length of the line segments is limited to a minimum length to avoid short segments. This minimum length can be modified from the configuration parameters to be suitable for all cases. When two or more elements are closer than the predefined minimum distance, the solver merge the models of the elements in a single element model that is split after the solution is obtained. Apart from that, all matrix operations use 64-bit floating point for high accuracy and the KLU linear solver is selected to solve the linear system described in Fig. 10 and in the eq. 22. KLU is specially designed to solve linear systems generated from the mathematical models of electric circuits and it can sort and scale the matrix to improve the accuracy of the solution [38]. It is designed to solve huge sparse matrices even under ill-condition. In our specific case we use the lower-upper (LU) factorization implemented in the above-mentioned KLU linear solver. In addition, it must be mentioned that off-course, all impedances and electrical variables use the per unit system in order to homogenize the values and improve the accuracy of the calculations.

At the initialization stage, the solver factorizes the (A) matrix into lower (L) and upper (U) matrices. During each iteration, the solver updates the (I_b) vector based on the nonlinear current model of the trains. Then, the linear system is solved by two steps of substitutions as shown in Equation 25. The lower triangle matrix is solved by forward substitution, while the backward substitution is used for solving the upper triangle matrix.

$$\begin{aligned} A \times x &= b & 1) \text{ Solve Forward: } L \times y &= b \\ L \times U \times x &= b & 2) \text{ Solve Backward: } U \times x &= y \end{aligned} \quad (25)$$

For the first iteration, the nodal voltages are initialized to the substation open circuit voltage. During the iterative process

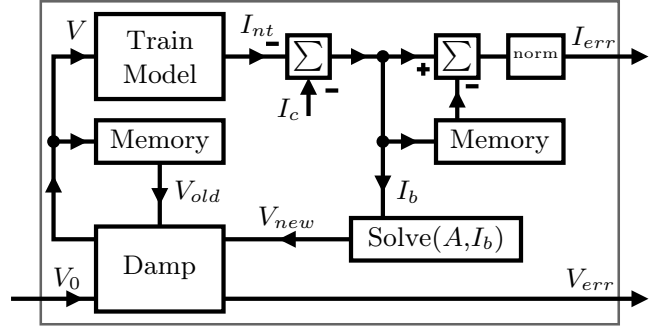


Fig. 10: Block diagram of the solver function

(summarized in Fig. 10), the nodal voltage is updated based on the adaptive damping algorithm represented in Fig. 11 to avoid oscillations and divergence.

The damping factor (D) forces the algorithm to select an intermediate point between the old (previous iteration) and new voltage (current iteration) as defined in Equation 26. This operation is performed in the "Damp" block of Fig. 10.

$$V = D \times V_{new} + (1 - D) \times V_{old} \quad (26)$$

The Damping factor may vary between 0.01 and 1. When ($D \approx 1$), the solver jumps directly to the new voltage which may improve the speed in normal cases. However, this condition may lead to divergence in critical cases. Low values of damping factor ($D < 0.01$) will slow down the convergence rate but the algorithm becomes more robust. The solver modifies the value of the damping factor dynamically based on the convergence rate.

The error of each iteration is estimated as a norm combination of the per unit difference error for the nodal voltage and the injection current as defined in Equation 27. The solver stops if the error is less than given tolerance. It must be remarked that the stopping criteria does not guaranty that the power absorbed or injected is the one defined in the XTP file as a reference power. However, we should also notice that the protection curves relating power with voltage are also embedded in the formulation as part of the model. If the voltage is between V_2 and V_3 (see Fig 7), the stopping criteria together with the equations provided by the curves guaranty that the power is equal to the reference power. In case that a voltage of a train is between V_1 and V_2 (Overcurrent protection activated) or between V_3 and V_4 (Overvoltage protection activated), the final result of the power will differ from the one specified in the XTP files as reference power, but this is the desired effect of the implementation of these protection curves.

$$Err = \underbrace{\|V_{new} - V_{old}\|}_{V_{err}} + \underbrace{\|I_{new} - I_{old}\|}_{I_{err}} \quad (27)$$

First, the solver initializes the damping factor to a low value ($D = 0.05$) to achieve a robust convergence rate in the first iterations. Then, the solver increases the damping factor gradually when the case has a smooth convergence rate to increase the convergence speed. The damping factor is reset to the initial value if the solver detects any overshoot or oscillation of the error. Equation 28 defines the convergence rate (r) as

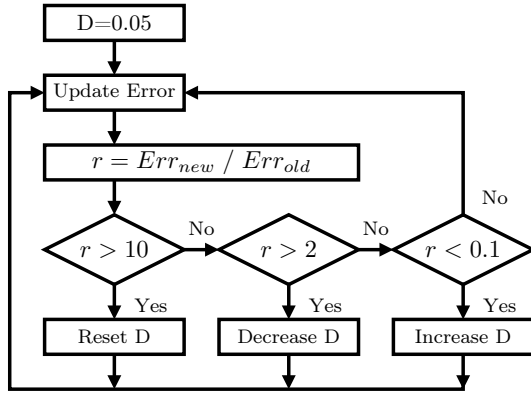


Fig. 11: Flow chart for updating the damping factor

a ratio between the errors of successive iterations.

$$r = \frac{Err_{new}}{Err_{old}} \quad (28)$$

The numerical limits shown in the flow chart of Fig. 11 are used to avoid overshooting and oscillation. Similar strategies have been applied to derivative based methods. For example, Levenberg-Marquardt method is known as damped least square method which is widely used for solving the nonlinear systems of equations [39], [40], [41]. However, it is not designed to deal with non-smooth characteristics like the ones introduced by the protection curves of the trains. In the following section, the performance of the proposed algorithm is compared with an improved version of the Levenberg-Marquardt algorithm.

IV. CASES OF STUDY

A. Test case of single section

Fig. 12 shows a simple network configuration of a single section with three cells and two parallel catenaries that share the same autotransformers and return conductor. The rails of the two tracks are electrically connected so it can be considered as an equivalent rail. The impedance parameters of this test case are listed on Table I based on the reference [22]. When the simulation starts, two trains from both terminals, connected to different catenaries are launched. Both trains travel through the section of 45km, the first one in forward direction and the second one in reverse direction. The section is divided in three cells, and as it can be observed in Fig. 12, the autotransformers are placed each 15km. The substation is a 20MVA substation with an output voltage in open circuit of ± 27.5 kV. The total resistance of the substation is 1128.75m Ω and the total inductance is 35.96mH. The impedance upstream the substation has been set to 4514.98m Ω and 143.71mH already referred to the 27.5kV voltage. Since the number of trains in the system is not elevated and in order to force the

Fig. 12: Topology of AC traction network

TABLE I: Impedance configuration of the test cases [22]

Z	R	L
Z_P	37.1 m Ω /km	0.43 mH/km
Z_G	22.9 m Ω /km	0.22 mH/km
Z_N	53.7 m Ω /km	0.63 mH/km

algorithm, we considered a multiplication factor of 2 for the impedance of the substation and a multiplication factor of 4 for the impedance of the positive, negative and ground feeders. We assume that the neutral point of the autotransformers is grounded with an impedance of 1 m Ω , higher ground impedances would provoke higher circulating currents in the rails of the sections without trains. As it can be observed the

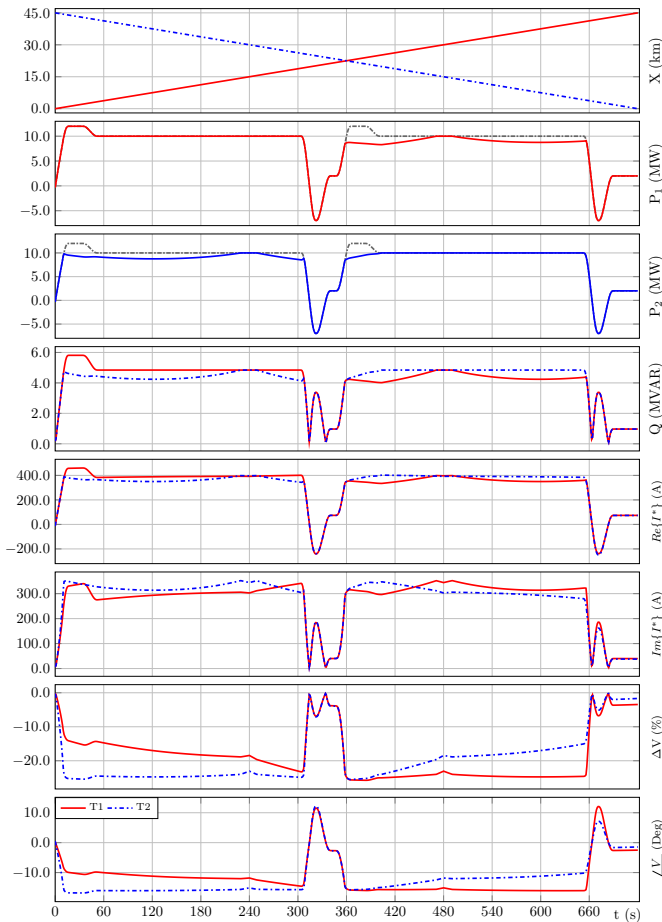


Fig. 13: The simulation results of the three trains test

model works fine even with a very small values of ground impedances in the autotransformers, however, solid grounding could cause ill conditioned systems. The voltages V_1 , V_2 , V_3 and V_4 of the protection curves has been set to 0.7, 0.76, 1.1 and 1.16 respectively (per unit values respect to 27.5kV). The simulation represents 720 instants at each second. Each instant is an individual network configuration based on trains position and power. The printed version of Fig. 12 shows a single instant at $t=360s$. However, the electronic version include the 720 instants. It is possible to interact with the graphical representation and select any of the 720 instants by means of the controls placed at the bottom of the figure.

In this case, the power profiles of all trains are generated by repeating patterns of acceleration and deceleration with intervals of constant power between them. In Fig. 13, the trains (T1 and T2) position, power, real and imaginary current, catenary voltage drop from the substation to the train and catenary voltage are represented. The peak power of the trains is 12 MW for acceleration and 7 MW for braking. The power factor has been set to 0.9 (lagging) for the whole simulation but it could be defined as a complex function depending on the active power reference. The actual power of the train is following nearly the same reference profile because the train voltage does not activate the protection curve in most of the instants. However, it must be observed that in some

occasions, the grey dashed line representing the reference power is different from the solid coloured line representing the actual power. In this specific case, this is because the overcurrent protection activation in a low voltage scenario. The real and imaginary components of the train conjugated current are represented in Fig. 13, the obtained profiles are highly correlated to the active and reactive power of the train.

The voltage deviation (ΔV) can reach 25% in some cases. The improvement of the voltage profile due to the autotransformer can be observed when the train passes at distances of 15 km and 30 km where the two first autotransformers are placed. The minimum voltage is caused by a peak demand power of more than 10 MW when the two trains are nearly in the middle of the section.

B. Performance test

The proposed method is tested using a computer generated network which includes 10 substations feeding a track of 1000 km divided into 20 sections of 50 km as shown in Fig. 14. Each section includes two catenaries and 5 cells of the same length and the same configuration as the one represented in Fig. 12 (two independent catenaries sharing the autotransformers and the return conductor with the rails electrically connected). A train is launched every ten minutes from both ends and the simulation include 18000 instants with time step 1 second.

Fig. 15 compares the performance of the proposed solver relative to LM (Levenberg-Marquardt) method based on the percent of solved cases relative to the total time. The proposed method takes less than 2 minutes to solve all instants while LM method requires around 30 minutes. Table II shows the results of the time per instant. Based on the average time per instant, the proposed method is more than 15 times faster than LM method with equivalent results and accuracy.

It must be remarked that this is not an algorithm to run in real time but for planning purposes, and because of that reason, CPU-time might not be critical. However, this solver is being used in real train and infrastructure manufacturer companies by the infrastructure design engineers. Before they get the final design of the network, they need to make thousands of simulations to check different network configurations, train schedules, and other different scenarios. It is important for them to have an agile tool in which they can make a variation in the system and obtain the new results in a fast way. For this reason, we think that it is important to develop not only accurate but also fast algorithms.

V. CONCLUSION

A simplified model for solving AC traction systems was presented in this paper, the model has been specifically

TABLE II: The time per instant of performance test

Time per instant	Proposed	LM
Minimum	1.85 ms	6.56 ms
Maximum	15.69 ms	422.92 ms
Mean	5.26 ms	99.60 ms
Standard Deviation	1.62 ms	88.71 ms

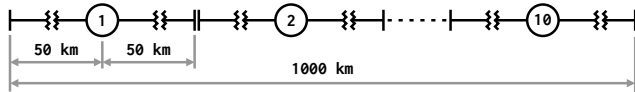


Fig. 14: A simplified diagram of 1000 km AC traction network

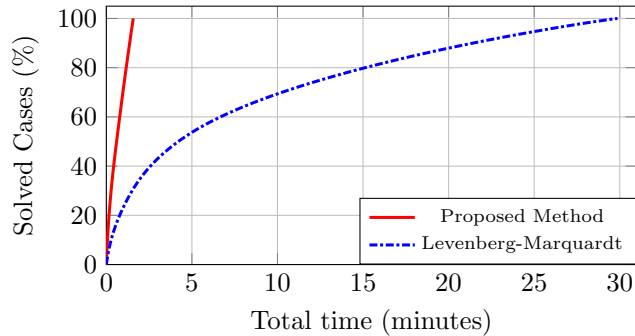


Fig. 15: Performance of the proposed method relative to Levenberg-Marquardt

designed for being used with bi-voltage high-speed traction systems but it can be also adapted for solving single-voltage AC systems. The solving procedure based on Modified Nodal Analysis (MNA) is faster than the derivative based solvers reaching the same level of accuracy. The implementation of the adaptive damping factor makes the algorithm very robust also in the presence of loads/generators with non-linear and non-smooth characteristics like the ones that the over-voltage and over-current protection of the trains add to the system.

REFERENCES

- [1] UITP International Association of Public Transport, from the French: L'Union internationale des transports publics, <http://www.uitp.org/>, Belgium, Europe, Founded in, 1885.
- [2] S. de la Torre, A. J. Sánchez-Racero, J. A. Aguado, M. Reyes, and O. Martínez, "Optimal sizing of energy storage for regenerative braking in electric railway systems," *IEEE Transactions on Power Systems*, vol. 30, no. 3, pp. 1492--1500, May 2015.
- [3] J. A. Aguado, A. J. S. Racero, and S. de la Torre, "Optimal operation of electric railways with renewable energy and electric storage systems," *IEEE Transactions on Smart Grid*, vol. 9, no. 2, pp. 993--1001, Mar. 2018.
- [4] A. Gomez-Exposito, J. M. Mauricio, and J. M. Maza-Ortega, "VSC-based MVDC railway electrification system," *IEEE Transactions on Power Delivery*, vol. 29, no. 1, pp. 422--431, Feb. 2014.
- [5] E. Pilo, S. K. Mazumder, and I. González-Franco, "Smart electrical infrastructure for AC-fed railways with neutral zones," *IEEE Transactions on Intelligent Transportation Systems*, vol. 16, no. 2, pp. 642--652, Apr. 2015.
- [6] Y. Sun, Z. Li, W. Tian, and M. Shahidehpour, "A lagrangian decomposition approach to energy storage transportation scheduling in power systems," *IEEE Transactions on Power Systems*, vol. 31, no. 6, pp. 4348--4356, Nov. 2016.
- [7] H. Hu, Z. He, K. Wang, X. Ma, and S. Gao, "Power-quality impact assessment for high-speed railway associated with high-speed trains using train timetable - part II: Verifications, estimations and applications," *IEEE Transactions on Power Delivery*, vol. 31, no. 4, pp. 1482--1492, Aug. 2016.
- [8] H. Hu, Z. He, X. Li, K. Wang, and S. Gao, "Power-quality impact assessment for high-speed railway associated with high-speed trains using train timetable - part I: Methodology and modeling," *IEEE Transactions on Power Delivery*, vol. 31, no. 2, pp. 693--703, Apr. 2016.
- [9] M. Brenna, F. Foiadelli, and D. Zaninelli, "Electromagnetic model of high speed railway lines for power quality studies," *IEEE Transactions on Power Systems*, vol. 25, no. 3, pp. 1301--1308, Aug. 2010.
- [10] Z. Liu, Z. Geng, and X. Hu, "An approach to suppress low frequency oscillation in the traction network of high-speed railway using passivity-based control," *IEEE Transactions on Power Systems*, vol. 33, no. 4, pp. 3909--3918, Jul. 2018.
- [11] R. A. Jabr and I. Džafić, "Solution of DC railway traction power flow systems including limited network receptivity," *IEEE Transactions on Power Systems*, vol. 33, no. 1, pp. 962--969, Jan. 2018.
- [12] P. Arboleya, B. Mohamed, and I. El-Sayed, "DC railway simulation including controllable power electronic and energy storage devices," *IEEE Transactions on Power Systems*, vol. 33, no. 5, pp. 5319--5329, Sep. 2018.
- [13] Y. Chen, R. White, T. Fella, S. Hillmansen, and P. Weston, "Multi-conductor model for AC railway train simulation," *IET Electrical Systems in Transportation*, vol. 6, no. 2, pp. 67--75, 2016.
- [14] E. Pilo, L. Rouco, A. Fernandez, and L. Abrahamsson, "A monovoltage equivalent model of bi-voltage autotransformer-based electrical systems in railways," *IEEE Transactions on Power Delivery*, vol. 27, no. 2, pp. 699--708, Apr. 2012.
- [15] M. Ceraolo, "Modeling and simulation of AC railway electric supply lines including ground return," *IEEE Transactions on Transportation Electrification*, vol. 4, no. 1, pp. 202--210, Mar. 2018.
- [16] B. Mohamed, P. Arboleya, and M. Plakhova, "Current injection based power flow algorithm for bilevel 2x25kV railway systems," in *2016 IEEE Power and Energy Society General Meeting (PESGM)*. IEEE, Jul. 2016.
- [17] S. V. Raygani, A. Tahavorgar, S. S. Fazel, and B. Moaveni, "Load flow analysis and future development study for an AC electric railway," *IET Electrical Systems in Transportation*, vol. 2, no. 3, pp. 139--147, Sep. 2012.
- [18] B. Mohamed, P. Arboleya, and C. González-Morán, "Modified current injection method for power flow analysis in heavy-meshed DC railway networks with nonreversible substations," *IEEE Transactions on Vehicular Technology*, vol. 66, no. 9, pp. 7688--7696, Sep. 2017.
- [19] S. Minucci, M. Pagano, and D. Proto, "Model of the 2x25kV high speed railway supply system taking into account the soil-air interface," *International Journal of Electrical Power and Energy Systems*, vol. 95, pp. 644--652, 2018.
- [20] M. Brenna and F. Foiadelli, "Sensitivity analysis of the constructive parameters for the 2x25kV high-speed railway lines planning," *IEEE Transactions on Power Delivery*, vol. 25, no. 3, pp. 1923--1931, Jul. 2010.
- [21] F. Kiessling, R. Puschmann, and A. Schmieder, *Contact lines for electric railways : planning, design, implementation*. Munich : Publicis, 2012.
- [22] A. Mariscotti, P. Pozzobon, and M. Vanti, "Simplified modeling of 2x25kV at railway system for the solution of low frequency and large-scale problems," *IEEE Transactions on Power Delivery*, vol. 22, no. 1, pp. 296--301, Jan. 2007.
- [23] P. Pan, H. Hu, X. Yang, F. Blaabjerg, X. Wang, and Z. He, "Impedance measurement of traction network and electric train for stability analysis in high-speed railways," *IEEE Transactions on Power Electronics*, vol. 33, no. 12, pp. 10086--10100, Dec. 2018.
- [24] H. Hu, H. Tao, F. Blaabjerg, X. Wang, Z. He, and S. Gao, "Train -- network interactions and stability evaluation in high-speed railways part I: Phenomena and modeling," *IEEE Transactions on Power Electronics*, vol. 33, no. 6, pp. 4627--4642, Jun. 2018.
- [25] Z. Liu, G. Zhang, and Y. Liao, "Stability research of high-speed railway EMUs and traction network cascade system considering impedance matching," *IEEE Transactions on Industry Applications*, vol. 52, no. 5, pp. 4315--4326, Sep. 2016.
- [26] H. Hu, H. Tao, X. Wang, F. Blaabjerg, Z. He, and S. Gao, "Train -- network interactions and stability evaluation in high-speed railways part II: Influential factors and verifications," *IEEE Transactions on Power Electronics*, vol. 33, no. 6, pp. 4643--4659, Jun. 2018.
- [27] Z. Liu and K. Hu, "A model-based diagnosis system for a traction power supply system," *IEEE Transactions on Industrial Informatics*, vol. 13, no. 6, pp. 2834--2843, Dec. 2017.
- [28] A. D'Ambrosio, N. Mijatovic, and V. G. Agelidis, "Lumped parameter model of a 2x25kV railway system based on root-matching method," in *2018 IEEE Transportation Electrification Conference and Expo, Asia-Pacific (ITEC Asia-Pacific)*, Jun. 2018, pp. 1--5.
- [29] M. Soler-Nicolau, J. Mera, J. López, and J. Cano-Moreno, "Improving power supply design for high speed lines and 2x25kV systems using a genetic algorithm," *International Journal of Electrical Power and Energy Systems*, vol. 99, pp. 309--322, 2018.
- [30] D. Serrano-Jiménez, L. Abrahamsson, S. Castaño-Solís, and J. Sanz-Feito, "Electrical railway power supply systems: Current situation and

future trends,” *International Journal of Electrical Power and Energy Systems*, vol. 92, pp. 181–192, 2017.

- [31] A. Dolara, M. Gualdoni, and S. Leva, “Impact of high-voltage primary supply lines in the 2×25 kV -- 50 Hz railway system on the equivalent impedance at pantograph terminals,” *IEEE Transactions on Power Delivery*, vol. 27, no. 1, pp. 164–175, Jan. 2012.
- [32] L. Battistelli, M. Pagano, and D. Proto, “ 2×25 kV - 50 Hz high-speed traction power system: Short-circuit modeling,” *IEEE Transactions on Power Delivery*, vol. 26, no. 3, pp. 1459–1466, Jul. 2011.
- [33] K. Mongkoldee and T. Kulworawanichpong, “Current-based Newton-Raphson power flow calculation for AT-fed railway power supply systems,” *International Journal of Electrical Power and Energy Systems*, vol. 98, pp. 11–22, 2018.
- [34] J. Zhang, M. Wu, and Q. Liu, “A novel power flow algorithm for traction power supply systems based on the Thévenin equivalent,” *Energies*, vol. 11, no. 1, 2018.
- [35] M. Brenna, F. Foiadelli, and D. Zaninelli, *Electrical Railway Transportation Systems*. IEEE Press, 2018.
- [36] I. E. Commission, “Railway applications - supply voltages of traction systems,” 2014.
- [37] E. C. for Electrotechnical Standardization, “Railway applications - supply voltages of traction systems,” 2004.
- [38] T. A. Davis and E. Palamadai Natarajan, “Algorithm 907: KLU, a direct sparse solver for circuit simulation problems,” *ACM Trans. Math. Softw.*, vol. 37, no. 3, pp. 36:1–36:17, Sep. 2010.
- [39] K. Levenberg, “A method for the solution of certain non-linear problems in least squares,” *Quarterly of applied mathematics*, vol. 2, no. 2, pp. 164–168, 1944.
- [40] M. L. A. Lourakis and A. A. Argyros, “Is Levenberg-Marquardt the most efficient optimization algorithm for implementing bundle adjustment?” in *Tenth IEEE International Conference on Computer Vision (ICCV'05) Volume 1*, vol. 2, Oct. 2005, pp. 1526–1531 Vol. 2.
- [41] P. J. Lagace, M. H. Vuong, and I. Kamwa, “Improving power flow convergence by Newton-Raphson with a Levenberg-Marquardt method,” in *2008 IEEE Power and Energy Society General Meeting - Conversion and Delivery of Electrical Energy in the 21st Century*, Jul. 2008, pp. 1–6.



Islam El-Sayed was born in Zagazig, Egypt, in 1984. He received the B.Sc. degree in electrical engineering from Zagazig University, Zagazig, in 2006. He received the Ph.D. degree in the Department of Electrical, Computer, and Systems Engineering, University of Oviedo, Gijón, Spain, in 2012. His ongoing research is connected with the application of bigdata, visual analytics and data driven documents to power systems analysis, modeling and simulation. Isla is responsible of front-end data analytics tools at LEMUR research group.



Bassam Mohamed received the M.Sc and Ph.D. degrees from the University of Oviedo, Gijón, Spain, in 2014 and 2018 respectively. He is now responsible of railway software development at LEMUR Research Group. His field of expertise has to do with the efficient development and implementation of algorithms for power systems analysis, specially those related to railway networks and unbalanced micro-grids. During the last years we developed several commercial software packages for electric network analysis and simulation.



Cristina González-Morán Cristina Gonzalez-Morn (SM15) received the M.Sc. and Ph.D. degrees from the University of Oviedo, Gijn, Spain, in 2003 and 2010, respectively, both in electrical engineering. She is currently an Associate Professor with the Department of Electrical Engineering, University of Oviedo, Gijn, Spain. She is the coordinator of the Electrical Energy Conversion and Power Systems Master Course. Her areas of interest include renewable energies, distributed generation and microgrids modeling, simulation, design, and optimization.



Pablo Arboleya (SM'13) received the M.Sc. and Ph.D. (with distinction) degrees from the University of Oviedo, Gijón, Spain, in 2001 and 2005, respectively, both in Electrical Engineering. Nowadays, he works as Associate Professor in the Department of Electrical Engineering at the University of Oviedo, he is Managing Editor of the *International Journal of Electrical Power and Energy Systems* and holder of the Gijón Smart Cities Chair at the University of Oviedo. Pablo is also Vice-Chair of IEEE Vehicular Technology Society Ad'Hoc Committee on Electric

Railway Systems. Presently his main research interests are focused in the micro-grid and smart-grid modeling and operation techniques, Internet of the Energy applications, railway traction networks simulation and combined AC/DC power flow algorithms.